

Fermi Surface Reconstruction inside the Hidden Order Phase of URu₂Si₂ Probed by Thermoelectric Measurements

Alexandre POURRET^{1*}, Alexandra PALACIO-MORALES¹, Steffen KRÄMER², Liam MALONE³,
Marc NARDONE², Dai AOKI^{1,4}, Georg KNEBEL^{1†}, and Jacques FLOUQUET¹

¹*SPSMS, UMR-E CEA / UJF-Grenoble 1, INAC, Grenoble, F-38054, France*

²*Laboratoire National des Champs Magnétiques Intenses, UPR CNRS 3228, CNRS - UJF- UPS - INSA, 25 rue des Martyrs, B.P. 166, 38042 Grenoble cedex 9 France and 143 avenue de Ranguéil, 31400 Toulouse, France*

³*H. H. Wills Physics Laboratory, University of Bristol, Tyndall Avenue, BS8 1TL, United Kingdom*

⁴*IMR, Tohoku University, Oarai, Ibaraki 311-1313, Japan*

We report thermoelectric measurements of the low carrier heavy fermion compound URu₂Si₂ at high fields up to 34T and at low temperatures down to 500mK. The field dependence of the thermoelectric power (TEP) and the Nernst signal shows successive anomalies deep inside the hidden order (HO) phase. The field position of these anomalies correspond to different changes in the Shubnikov-de Haas frequencies and effective masses around 12 T, 17 T, 23 T and 30 T. These results indicate successive reconstructions of the Fermi surface, which imply electronic phase transitions well within the HO phase.

KEYWORDS: Hidden Order, URu₂Si₂, Thermoelectric power, Nernst effect

1. Introduction

The nature of the so-called hidden order (HO) state of the low carrier heavy fermion compound URu₂Si₂ below the second order phase transition at $T_0 = 17.5$ K is still under debate. The electronic structure changes significantly at the transition from the paramagnetic (PM) to the HO state. Various experimental probes show the gap opening on the Fermi surface below T_0 and most of the charge carriers disappear resulting in a semimetallic state.^{1,2} Angular-resolved photoemission spectroscopy observes a narrow dispersive band emerging in the HO state.^{3,4} The opening of a hybridization gap at T_0 has been shown by recent scanning tunneling microscopy experiment.^{5,6} At low temperature, the remaining small numbers of carriers undergo a transition into an unconventional superconducting state at $T_{sc}=1.5$ K.⁷⁻⁹ Recently several exotic order parameters have been proposed for the HO phase including various rank multipole order,¹⁰⁻¹³ dynamical symmetry breaking,^{14,15} spin-nematic states¹⁶ or hastatic order,¹⁷ among others. No higher ordered multipole has been detected by scattering experiments, however dotriacontapole ordering has been proposed from macroscopic experiments, recently.^{18,19}

The HO is affected by external parameters, such as pressure and magnetic field. Above the critical pressure of $P_x \approx 0.5$ GPa, a long range antiferromagnetic ordered state with large moments ($\approx 0.4\mu_B/U$) emerges,^{20,21} but no dramatic modification of the Fermi surface is reported between the HO and antiferromagnetic phases.^{22,23} In contrast, a strong magnetic field applied along the easy c axis of this tetragonal crystal destroys the HO phase at $H_c \approx 35$ T accompanying a radical reconstruction of the Fermi surface.²⁴⁻²⁷ Above H_c a cascade of several unknown phases are observed just below the metamagnetic

field $H_M \approx 39$ T where a polarized paramagnetic (PPM) metal with large carrier number is recovered.^{28,29}

While inside the HO phase ($H < 35$ T for $H||c$) no sign of a phase transition can be detected in macroscopic thermodynamic measurements such as the magnetization or the specific heat, topological changes of the Fermi surface (FS) are observed. The first evidence for such FS modifications have been reported by the observation of a new quantum oscillation frequency in the Hall effect slightly below $H^* = 23$ T.³⁰ Furthermore, a cascade of FS singularities below H_c have been emphasized from the field dependence of the Shubnikov de Haas (SdH) frequencies.^{23,27,31} Thermoelectric power (TEP) is known as a very sensitive probe of electronic instabilities and it is a sound approach to study in detail its corresponding response. Recently, TEP has confirmed the singularity at $H^* = 23$ T and suggested also another anomaly at already $H_m \approx 10$ T.³²

In this paper we present a new generation of thermoelectric experiments, extending our previous measurements down to $T \sim 500$ mK and from $H = 28$ T to 34 T, very close to H_c . We observe various anomalies in TEP and in the Nernst signal (N) inside the HO state. They are marks of a successive Fermi surface evolution deep inside the HO phase. Thus, they establish a clear reference between FS changes and its consequences on transport properties.

2. Experimental details

High-quality single crystals were grown using the Czochralski pulling method in a tetra-arc furnace. Two different samples have been used. Sample 1 ($J||a$, $H||c$ configuration in the tetragonal crystal structure) had a residual resistance ratio (RRR) of 100, sample 2 ($J||H||c$ configuration) had RRR of 50. The TEP was measured using the standard "one heater-two thermometer" setup. Measurements up to 34 T and down to 500 mK were per-

*E-mail address: alexandre.pourret@cea.fr

†E-mail address: georg.knebel@cea.fr

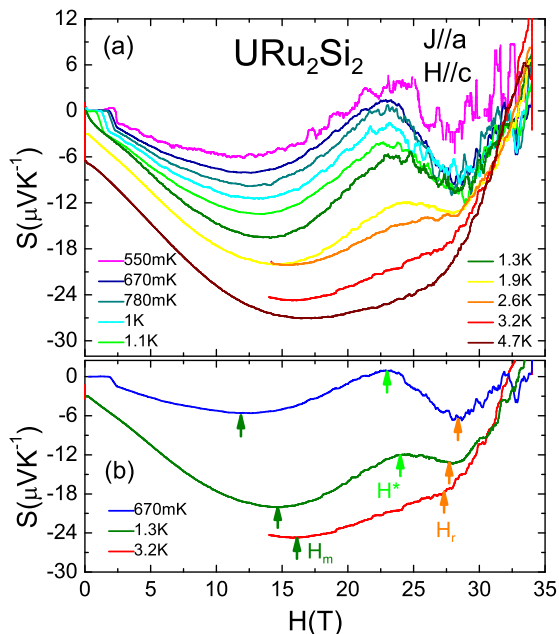


Fig. 1. (Color online) (a) Thermoelectric power S of URu_2Si_2 for $J\parallel a$ and $H\parallel c$ as a function of magnetic field for different temperatures. (b) Different anomalies extracted from the TEP and followed as function of temperature: H_m corresponds to the minimum of the thermoelectric power, H^* and H_r corresponds to the local maximum and minimum of the thermoelectric power at high field.

formed in a resistive magnet at the Laboratoire National des Champs Magnetiques Intenses (LNCMI) Grenoble using a recently developed ^3He probe. A significant increase of the noise level had been observed for fields above 20 T which is mainly a consequence of vibrations caused by the water-cooling of the magnet. Thus, curves are slightly smoothed for clarity.

3. Results

Figure 1(a) shows the TEP as a function of magnetic field up to 34 T for different temperatures. The field is applied along the c axis and the heat current J along the a axis. S is negative revealing an heavy electron band as the dominant heat carrier in the system in the normal state above H_{c2} while the Hall effect is dominated by a light hole Fermi surface.⁷ As a function of magnetic field, S shows successive anomalies at low temperature, clearly defined in Fig. 1(b): a rather broad minimum at $H_m \sim 11$ T followed by an increase and a local maximum at $H^* \sim 23$ T and finally another minimum around $H_r \sim 30$ T.³¹ With increasing temperature both, H_m and H^* increase in field while H_r decreases and the anomalies at H^* and H_r get apparently smeared out. Above $T \approx 3$ K, well below the critical temperature corresponding to the critical field H_c of the HO phase, the anomalies can no longer be clearly resolved. The field dependence is in good agreement with the previous report.³²

The Nernst signal ($J\parallel a, H\parallel c$) measured simultaneously on the same sample as the TEP is shown in Fig. 2(a). At high temperature, i.e at $T = 4.7$ K and 6.7 K, we observe the same field dependence as reported in previous measurements performed in pulsed magnetic field:²⁶ the

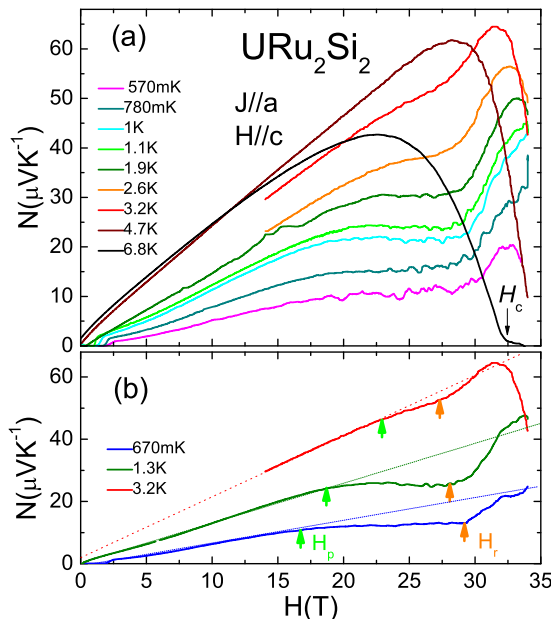


Fig. 2. (Color online) (a) Nernst signal of URu_2Si_2 for $J\parallel a$, $H\parallel c$ as a function of magnetic field for different temperatures. H_c indicates the critical field above which the HO is suppressed. (b) The different anomalies extracted from the Nernst signal: H^* corresponds to the field position where the Nernst signal moves away from a linear field dependence, H_r is linked to the abrupt increase of the Nernst signal at high field.

Nernst signal increases almost linearly with the magnetic field, reaches a large maximum and decreases to zero at H_c when the HO is suppressed. The low carrier number (small Fermi surfaces) in addition to the high mobility of the charge carriers explains the existence of such a large Nernst signal in the HO phase (N reaches $65 \mu\text{V}\text{K}^{-1}$ at 32 T and 3.2 K). In the PM regime, above H_c , the Nernst effect is almost zero. This extremely large value of the Nernst signal appears to be an intrinsic property of the HO. However, additional anomalies in the $N(H)$ appear below 3.2 K. $N(H)$ is almost linear up to a field $H_p \sim 17$ T. But for higher fields strong deviations from linearity are observed at low temperature. The field dependence suggests an additive negative contribution to the Nernst signal above H_p getting more and more pronounced on lowering temperature. For $H > H_r$ a sudden increase of the Nernst signal appears and the signal reaches the value from the linear extrapolation from low fields. The positions of the anomalies observed in the field dependence of the Nernst signal are defined in Fig. 2(b). Again, these anomalies suggest a change in the relative weight of the dominant heat carriers with increasing magnetic field up to H_c .

Previously, strong differences in the field dependence of the transverse and the longitudinal magnetoresistance had been reported.²⁹ While the transverse magnetoresistance shows a strong field dependence with a huge maximum at $H_{\rho max} \approx 30$ T,²⁹ strongly dependent on the sample quality and dominated by the cyclotron motion of the charge carriers, the longitudinal magnetoresistance does not show such a strong field dependence in the HO state. Thus, we also performed TEP measurements in the

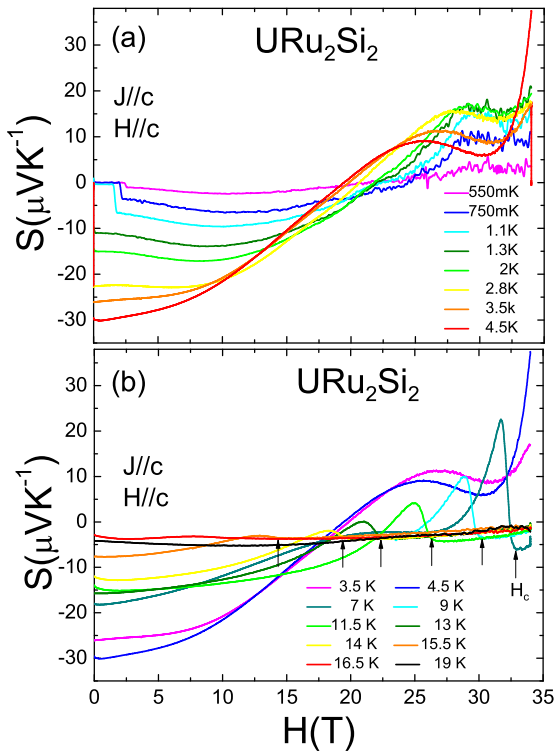


Fig. 3. (Color online) TEP of URu_2Si_2 for $J \parallel c, H \parallel c$ as a function of magnetic field for (a) low temperatures and (b) high temperatures. Above 4.5 K, S presents a peak below the critical field H_c (defined by vertical arrows) and in the PM state for $H > H_c$, S is field independent.

longitudinal configuration ($J \parallel H \parallel c$), shown in Fig. 3. In the paramagnetic state for $T > T_0$ the signal is negative and small up to the highest field. Above 4.5 K we clearly see a peak in the TEP just below the critical field H_c and in the PM state for $H > H_c$, S is field independent. With lowering the temperature the peak gets more and more pronounced. At low temperature $T < 4.5$ K, similar anomalies of the TEP in this longitudinal configuration as in the transverse configuration discussed above can be noticed, but the respective anomalies seem to be shifted to slightly higher fields compared to the transverse configuration. This aspect indicates that the anomalies observed in the different thermoelectric effects are not only governed by scattering but are a direct consequence of successive instabilities of different Fermi surface pockets at low temperature just below H_c .

4. Discussion

Next, we will compare the thermoelectric response to the field dependent resistivity results.^{23,27,31} Fig. 4(a) shows TEP and Nernst signal at 1 K and (b) the transverse magnetoresistance $\rho(H)$ for $H \parallel c$ and $J \parallel a$ at $T = 30$ mK as function of field up to 34 T taken from refs. 23, 31. In the magnetoresistance three different anomalies occurs in the raw data, a tiny kink at $H_k \sim 8.5$ T, a second kink with strong enhancement at $H^* \sim 23$ T and a maximum at $H_r \sim 30$ T. The non-oscillatory part of $\rho(H)$ follows a H^2 dependence up to 8 T and in a second regime from 9 T to almost 17 T. A H^2 dependence is expected for the transverse mag-

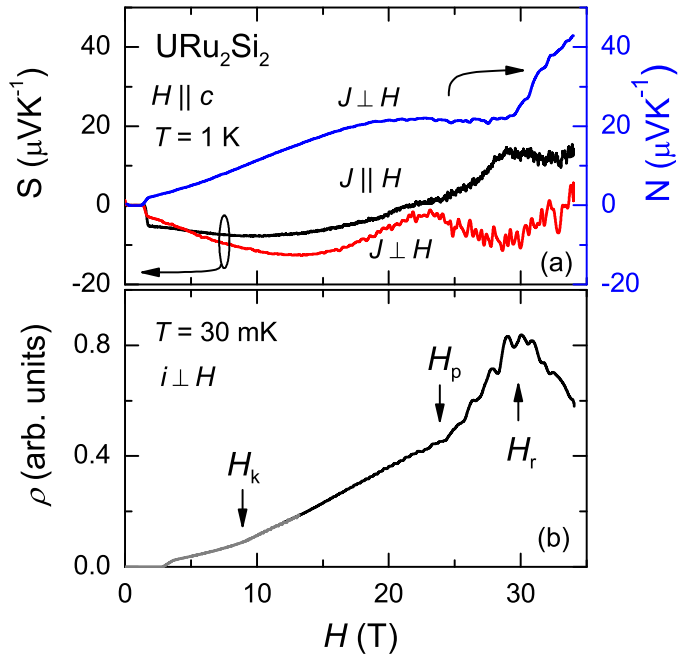


Fig. 4. (Color online). (a) TEP and Nernst signal obtained at $T = 1$ K. (b) Transverse magnetoresistance for $H \parallel c$ at 30 mK: (grey line) from ref. 23, (black line) ref. 31. The arrows indicate the position of anomalies observed in the previous magnetoresistivity experiments.

netoresistance in an compensated metal.³³ Clearly, the field ranges of the thermoelectric anomalies correspond to changes in the magnetoresistance.

To summarize the experimental data of successive anomalies inside the hidden order phase, the different anomalies observed in the TEP (full symbol) and in the Nernst signal (open symbol), mentioned above, are reported in the $H - T$ phase diagram for $H \parallel c, J \parallel a$ in Fig. 5. Using the TEP in the longitudinal configuration, positions of the field independent TEP (black square) delimiting the HO state are reported. Furthermore, we added the anomalies in the Hall resistance shown in Fig. 1 (b) of ref. 30 (half-filled square). As shown in that figure, the Hall effect shows two maxima as function of field, labelled H_p and H^* . (In difference to ref. 30 we plot in the phase diagram both, H_p and H^* . We define these characteristic fields as the maxima in the Hall signal ρ_{xy} , while in the ref.³⁰ H^* is defined as inflection point in ρ_{xx} or in the second derivative $d^2\rho_{xy}/dH^2$). That's why the curvature of $H^*(T)$ plotted here is opposite to that in the original paper.) In addition we also plot the maximum of resistivity at H_r taken from in ref. 29) (half-filled circle, in that paper labelled $H_{\rho,max}$). The transport experiments give evidence for several anomalies inside the HO state, while thermodynamic probes do not show any phase line. Furthermore, it should be noticed that all anomalies detected inside the HO state get smeared out for $T > 3$ K indicating that they are not conventional phase transitions but related to electronic instabilities of the Fermi surface.

On the basis SdH experiments a successive polarization of different Fermi surface pockets has been discussed.^{23,27,31} Thus, the field position of the succes-

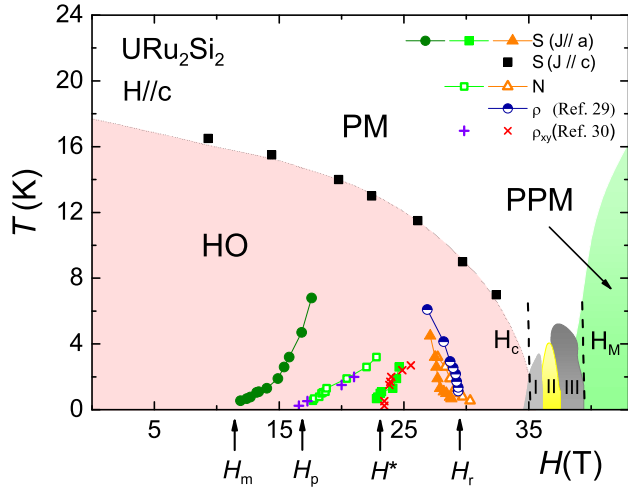


Fig. 5. (Color online) $H-T$ Phase diagram of URu_2Si_2 . Several anomalies have been observed inside the HO phase. Full symbols mark anomalies observed in TEP for $H\parallel a$ (circles, squares, triangle) and $J\parallel c$ (black squares). Anomalies in the Nernst signal are indicated by open symbols. Furthermore, we include anomalies observed in the Hall resistance ρ_{xy} taken from ref. 30 (plus and cross). The indicated anomalies correspond to the maxima in ρ_{xy} vs H of Fig. 1(b) of ref. 30. The maximum of resistivity at H_r ²⁹ (half-filled circle) are also included. The field position of the successive changes in the SdH frequencies (H_p , H^* , H_r) are indicated by vertical arrows (see text).³¹ H_m corresponds to the broad minimum in the TEP. Finally, the different phases which occur between H_c and H_M (I, II, III) and the polarized paramagnetic (PPM) state are indicated.^{28,29} This part of the phase diagram was not reached in this report.

sive changes in the SdH frequencies (H_p , H^* , H_r) are indicated by vertical arrows in the phase diagram.³¹ The small Fermi surfaces with heavy masses are more easily affected by magnetic field. These changes give strong feedback on the thermoelectric response. H_m corresponds to the broad minimum in the TEP.

Finally we look closer to the previously observed field dependence of the SdH frequencies and the effective cyclotron masses as summarized in Fig. 6. In URu_2Si_2 , several bands have been observed by quantum oscillations.³¹ Four main quantum oscillation frequencies are observed at low field α , β , γ , and η with frequencies $F = 1.05$, 0.42 , 0.19 , and 0.09 kT, respectively.^{23,35} The α sheet is most likely attributed to a largest hole Fermi surface centered at the Γ point in the simple tetragonal Brillouin zone, β is a four-fold electron Fermi surface located between Γ and X points, γ and η are small Fermi surface at the M and Z point, respectively. All quantum oscillation experiments miss a heavy electron Fermi surface which is located at the M point. Possibly, this branch may have been observed in recent cyclotron resonance experiments.³⁶

Significant changes of the SdH frequencies and the effective masses m^* appear under magnetic field as shown in Fig. 6 (a) and (b). It is obvious that in this highly correlated multiband system a modification of one band has strong feedback to all other bands, as at least in the HO state, URu_2Si_2 is low carrier compensated metal. As discussed in refs. 32 and 27 the characteristic energies for each band are very low and can be simply estimated by

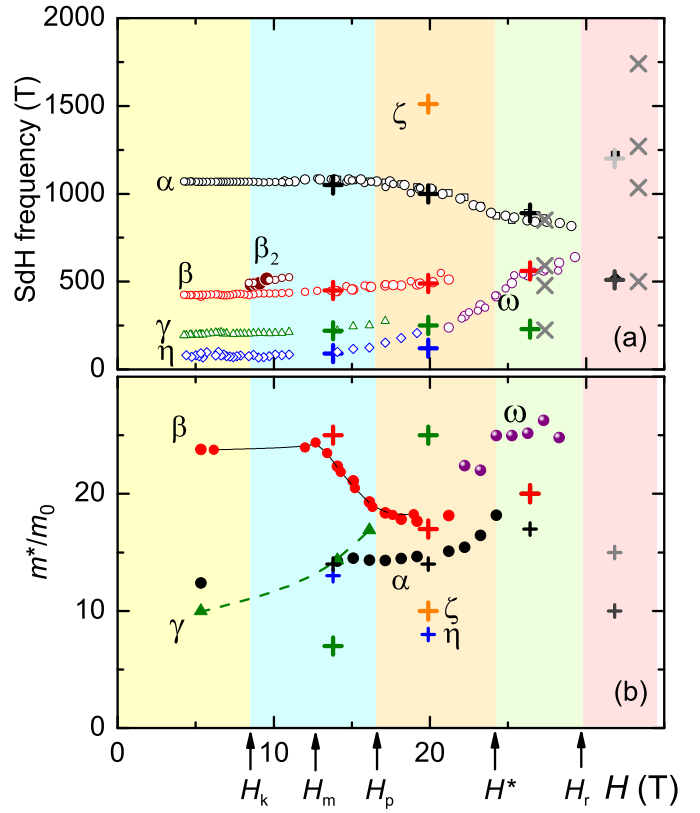


Fig. 6. (Color online). (a) Field dependence of the SdH frequencies in the different field ranges. Small open symbols are from ref. 23 and 31, large pluses are taken from ref. 27, large crosses from ref. 34. The different magnetic field positions H_k , H_m , H_p , H^* and H_r are indicated by vertical arrows (see text).

$\Delta_f = \frac{\hbar e F}{m^* k_B}$. Thus the magnetic fields to fully polarize the bands is rather low and we can estimate that for a field of 20 T all bands except the larger α branch would be polarized.²⁷ A first change in the field dependence of the SdH frequencies appears already at relatively small $H_k \approx 8$ T where the magnetoresistance shows a small kink and the spin split of the β branch appears.²³ This anomaly in the magnetoresistance is smeared out already at $T \sim 100$ mK. The observed broad minimum in the transverse TEP at H_m appears at $T \sim 500$ mK at slightly higher fields than H_k . In the field range of H_m a strong decrease of the effective mass of the β branch is observed (see fig.6(b)). In a multi-band system like URu_2Si_2 , the total Seebeck coefficient S is given by the sum of Seebeck coefficient of each band S_i weighted by its respective conductivity, $S = \sum_i S_i \sigma_i / \sigma$. In difference to conductivity the Seebeck effect can have positive and negative sign, thus the sum of the overall Seebeck effect can be smaller than the contribution of each band. The broad minimum at H_m can be understood as the balance of two different contributions to the TEP. While at low field $H < H_m$ the electron contribution dominates, above H_m a positive hole contribution start to increase as the mass of the electron pocket starts to decrease.

A smooth decrease of the frequency of the α branch starts above 15 T and reaches nearly 820 T at $H \sim 29$ T (a reduction of about 20 %). In this field region the TEP increases up to H^* . This supports the interpretation of

the enhancement of the hole contribution in the thermoelectric response, as the mass of observed electron band β gets lighter, and vice versa the mass of the hole band α increases slightly. Above $H_p \sim 17$ T the appearance of an additional frequency ϵ has been reported in Hall effect measurements,³⁰ however it has never been reproduced in SdH or de Haas van Alphen experiments. The effective mass of this ϵ branch is very low ($m_\epsilon = 2.3 m_0$). This field coincides with the anomaly in the Nernst signal, while no signature appears in the Seebeck effect. Strong field induced modifications of the Fermi surface emerges clearly at H^* and at H_r . At H^* we previously detected the appearance of a new branch named ω with large cyclotron mass.³¹ In the field range from $H^* \approx 23$ T to $H_r \approx 30$ T, this new branch coexists at least with the α branch, while an abrupt change of all frequencies appear above H_r . We observe in the limited field range from H_r up to H_c new frequencies in accordance to refs. 27, 34. Remarkably, the sharp anomalies we observed in the thermoelectric response correspond to changes in the Fermi surface topology. In this multiband system magnetic field modifies the balance of the electron and hole contributions to TEP and Nernst effect critically as well as modifications of the Fermi surface topology due to Lifshitz transitions. At $T = 0$, these give rise to a diverging TEP,³² while the experiments are performed at finite temperature and the divergences are smeared out.

5. Summary

In conclusion, the field dependence of the TEP and the Nernst signal in URu₂Si₂ shows successive anomalies deep inside the HO phase. The field position of these anomalies correspond to different changes in the SdH frequencies around 12 T, 23 T and 30 T. These results indicate successive reconstructions of the Fermi surface, which imply electronic phase transitions well within the HO phase. The origin of the phenomena is the Zeeman splitting of the different Fermi sheets. The fact that the TEP anomalies at finite temperature are rather broad appears to be the mark of the strong interplay between the different Fermi sheet. A sharper TEP anomaly has been observed in CeRu₂Si₂ at its pseudometamagnetic transition associated with drastic change of the Fermi surface.^{37, 38} The present work gives a new fact of the link between Fermi surface reconstruction and TEP response in the complex matter of strongly correlated electronic systems.

Acknowledgements

We thank G. Scheerer, W. Knafo and H. Harima for many useful discussions. This work has been supported by the French ANR (projects PRINCESS, SINUS, CORMAT, DELICE), the ERC (starting grant NewHeavyFermion), the EuromagNET II (EU contract no. 228043) and the Université Grenoble-1 within the Pole SMINGUE.

- 1) R. Bel, H. Jin, K. Behnia, J. Flouquet, and P. Lejay: Phys. Rev. B **70** (2004) 220501.
- 2) K. Behnia, R. Bel, Y. Kasahara, Y. Nakajima, H. Jin, H. Aubin, K. Izawa, Y. Matsuda, J. Flouquet, Y. Haga, Y. Onuki, and P. Lejay: Phys. Rev. Lett. **94** (2005) 156405.
- 3) A. F. Santander-Syro, M. Klein, F. L. Boariu, A. Nuber, P. Lejay, and F. Reinert: Nat. Phys. **5** (2009) 637.
- 4) R. Yoshida, Y. Nakamura, M. Fukui, Y. Haga, E. Yamamoto, Y. Onuki, M. Okawa, S. Shin, M. Hirai, Y. Muraoka, and T. Yokoya: Phys. Rev. B **82** (2010) 205108.
- 5) P. Aynajian, E. H. da Silva Neto, C. V. Parker, Y. Huang, A. Pasupathy, J. Mydosh, and A. Yazdani: Proc. Natl. Acad. Sci. U. S. A. **107** (2010) 10383.
- 6) A. R. Schmidt, M. H. Hamidian, P. Wahl, F. Meier, a. V. Balatsky, J. D. Garrett, T. J. Williams, G. M. Luke, and J. C. Davis: Nature **465** (2010) 570.
- 7) Y. Kasahara, T. Iwasawa, H. Shishido, T. Shibauchi, K. Behnia, Y. Haga, T. Matsuda, Y. Onuki, M. Sigrist, and Y. Matsuda: Phys. Rev. Lett. **99** (2007) 116402.
- 8) R. Okazaki, Y. Kasahara, H. Shishido, M. Konczykowski, K. Behnia, Y. Haga, T. Matsuda, Y. Onuki, T. Shibauchi, and Y. Matsuda: Phys. Rev. Lett. **100** (2008) 037004.
- 9) K. Yano, T. Sakakibara, T. Tayama, M. Yokoyama, H. Amitsuka, Y. Homma, P. Miranović, M. Ichioka, Y. Tsutsumi, and K. Machida: Phys. Rev. Lett. **100** (2008) 017004.
- 10) K. Haule and G. Kotliar: Nature Physics **5** (2009) 796.
- 11) H. Kusunose: J. Phys. Soc. Jpn. **81** (2012) 023704.
- 12) H. Ikeda, M.-T. Suzuki, R. Arita, T. Takimoto, T. Shibauchi, and Y. Matsuda: Nat. Phys. **8** (2012) 528.
- 13) J. G. Rau and H. Y. Kee: Physical Review B **85** (2012) 245112.
- 14) S. Elgazzar, J. Ruzs, M. Amft, P. M. Oppeneer, and J. a. Mydosh: Nat. Mater. **8** (2009) 337.
- 15) P. Oppeneer, J. Ruzs, S. Elgazzar, M.-T. Suzuki, T. Durakiewicz, and J. Mydosh: Phys. Rev. B **82** (2010) 205103.
- 16) S. Fujimoto: Phys. Rev. Lett. **106** (2011) 196407.
- 17) P. Chandra, P. Coleman, and R. Flint: ArXiv e-prints (2012) 1207.4828.
- 18) R. Okazaki, T. Shibauchi, H. J. Shi, Y. Haga, T. D. Matsuda, E. Yamamoto, Y. Onuki, H. Ikeda, and Y. Matsuda: Science (New York, N.Y.) **331** (2011) 439.
- 19) E. Ressouche, R. Ballou, F. Bourdarot, D. Aoki, V. Simonet, M. T. Fernandez-Diaz, A. Stunault, and J. Flouquet: Phys. Rev. Lett. **109** (2012) 067202.
- 20) H. Amitsuka, K. Matsuda, I. Kawasaki, K. Tenya, M. Yokoyama, C. Sekine, N. Tateiwa, T. Kobayashi, S. Kawarazaki, and H. Yoshizawa: J. Magn. Magn. Mater. **310** (2007) 214.
- 21) E. Hassinger, G. Knebel, K. Izawa, P. Lejay, B. Salce, and J. Flouquet: Phys. Rev. B **77** (2008) 115117.
- 22) M. Nakashima, H. Ohkuni, and Y. Inada: J. Phys.: Condens. Matter **15** (2003) 2011.
- 23) E. Hassinger, G. Knebel, T. Matsuda, D. Aoki, V. Taufour, and J. Flouquet: Phys. Rev. Lett. **105** (2010) 216409.
- 24) M. Jaime, K. Kim, G. Jorge, S. McCall, and J. Mydosh: Phys. Rev. Lett. **89** (2002) 287201.
- 25) J. Kim, D. Hall, P. Kumar, and G. Stewart: Phys. Rev. B **67** (2003) 01440.
- 26) J. Levallois, K. Behnia, and J. Flouquet: EPL **85** (2009) 27003.
- 27) M. M. Altarawneh, N. Harrison, S. E. Sebastian, L. Balicas, P. H. Tobash, J. D. Thompson, F. Ronning, and E. D. Bauer: Phys. Rev. Lett. **106** (2011) 146403.
- 28) K. Kim, N. Harrison, M. Jaime, G. Boebinger, and J. Mydosh: Phys. Rev. Lett. **91** (2003) 256401.
- 29) G. W. Scheerer, W. Knafo, D. Aoki, G. Ballou, A. Mari, D. Vignolles, and J. Flouquet: Phys. Rev. B **85** (2012) 094402.
- 30) H. Shishido, K. Hashimoto, T. Shibauchi, T. Sasaki, H. Oizumi, N. Kobayashi, T. Takamasu, K. Takehana, Y. Imanaka, T. Matsuda, Y. Haga, Y. Onuki, and Y. Matsuda: Phys. Rev. Lett. **102** (2009) 156403.
- 31) D. Aoki, G. Knebel, I. Sheikin, E. Hassinger, L. Malone, T. D. Matsuda, and J. Flouquet: J. Phys. Soc. Jpn. **81** (2012) 074715.
- 32) L. Malone, T. Matsuda, A. Antunes, G. Knebel, V. Taufour, D. Aoki, K. Behnia, C. Proust, and J. Flouquet: Phys. Rev. B **83** (2011) 245117.
- 33) A. B. Pippard: *Magnetoresistance in Metals* (Cambridge Uni-

1) R. Bel, H. Jin, K. Behnia, J. Flouquet, and P. Lejay: Phys. Rev. B **70** (2004) 220501.

2) K. Behnia, R. Bel, Y. Kasahara, Y. Nakajima, H. Jin,

- versity Press, Cambridge, U.K., 1989).
- 34) Y. Jo, L. Balicas, C. Capan, K. Behnia, P. Lejay, J. Flouquet, J. Mydosh, and P. Schlottmann: *Phys. Rev. Lett.* **98** (2007) 166404.
- 35) H. Ohkuni, Y. Inada, Y. Tokiwa, K. Sakurai, R. Settai, T. Honma, Y. Haga, E. Yamamoto, Y. Onuki, H. Yamagami, S. Takahashi, and T. Yanagisawa: *Philos. Mag. B* **79** (1999) 1045.
- 36) S. Tonegawa, K. Hashimoto, K. Ikada, Y.-H. Lin, H. Shishido, Y. Haga, T. Matsuda, E. Yamamoto, Y. Onuki, H. Ikeda, Y. Matsuda, and T. Shibauchi: *Phys. Rev. Lett.* **109** (2012) 036401.
- 37) A. Amato, D. Jaccard, J. Sierro, P. Haen, P. Lejay, and J. Flouquet: *J. Low Temp. Phys.* **77** (1989) 195.
- 38) H. Pfau, R. Daou, M. Brando, and F. Steglich: *Phys. Rev. B* **85** (2012) 035127.